Photophysical properties of hexa-functionalized C_{60} derivatives: Spectroscopic and quantum-chemical investigations

P.-F. Coheur
Laboratoire de Chimie Physique Moléculaire, Université Libre de Bruxelles, CP 160/09, 50 Avenue F.D. Roosevelt, B-1050 Brussels, Belgium

J. Cornil and D. A. dos Santos
Service de Chimie des Matériaux Nouveaux, Centre de Recherche en Electronique et Photonique Moléculaires, Université de Mons-Hainaut, Place du Parc 20, B-7000 Mons, Belgium

P. R. Birkett
Fullerene Science Centre, CPES School, University of Sussex Brighton, BN1 9QJ, United Kingdom

J. Liévin
Laboratoire de Chimie Physique Moléculaire, Université Libre de Bruxelles, CP 160/09, 50 Avenue F.D. Roosevelt, B-1050 Brussels, Belgium

J. L. Brédas
Service de Chimie des Matériaux Nouveaux, Centre de Recherche en Electronique et Photonique Moléculaires, Université de Mons-Hainaut, Place du Parc 20, B-7000 Mons, Belgium and Department of Chemistry, The University of Arizona, Tucson, Arizona 85721-0041

D. R. M. Walton, R. Taylor, and H. W. Kroto
Fullerene Science Centre, CPES School, University of Sussex Brighton, BN1 9QJ, United Kingdom

R. Colin[a)]
Laboratoire de Chimie Physique Moléculaire, Université Libre de Bruxelles, CP 160/09, 50 Avenue F.D. Roosevelt, B-1050 Brussels, Belgium

(Received 13 December 1999; accepted 11 February 2000)

The photophysical properties of hexa-functionalized C_{60} derivatives ($C_{60}Cl_6$, $C_{60}Ph_5Cl$, $C_{60}Ph_5H$, and two $C_{60}Ph_5OH$ isomers) have been investigated by means of UV–visible absorption and fluorescence spectroscopy in cyclohexane solution and quantum-chemical calculations derived from semiempirical Hartree–Fock approaches. A very good agreement is obtained between the measured absorption and fluorescence spectra and the calculated excitation energies, thus allowing for a detailed assignment of the optical features. The effects of symmetry and chemical nature of the functional groups on the ground-state and spectroscopic properties of the C_{60} derivatives are discussed. © *2000 American Institute of Physics.* [S0021-9606(00)01617-2]

I. INTRODUCTION

The physical properties of the fullerenes C_{60} and C_{70} have been extensively studied in recent years and some have proved to be of a particular interest, which may result in applications in the fields of either material sciences or biomedicine. The use of fullerenes as optical limiters[1] or O_2 photosensitizers[2,3] has in particular attracted much attention. Such usage relies on the photophysical processes characteristic of the fullerenes that have been recently reviewed by Sun.[4] As a result of the low solubility of the fullerenes in water and the difficulty encountered in incorporating them into host materials it is expected that fullerene derivatives will find most use in this area of research. Several functionalized derivatives of C_{60} and C_{70} have already been shown to have retained the majority of the useful photophysical characteristics of the parent molecules yet they avoid some of the foregoing problems; this is especially true for the nonlinear absorptive properties[5–9] and efficient generation of $O_2(^1\Delta_g)$[10–16] of some derivatives.

Functionalized fullerenes can be prepared under a variety of reaction conditions.[17–19] The most frequently encountered and studied compounds are monofunctionalized cycloadducts of C_{60}, such as methano- or pyrrolidino-C_{60}. The distinctive spectroscopic features of these monofunctionalized derivatives have been thoroughly characterized.[4–7,10–13,20–26] By contrast, the spectroscopy of multifunctional C_{60} derivatives has not been investigated to the same extent.[10,16,20,21,27–31] This information might prove, however, to be valuable in determining how the perturbation of the π-electronic system influences the ground- and excited-state properties of the fullerene cages. Furthermore, with the exception of the work on pseudodihydro-C_{60} derivatives achieved by Udvardi *et al.*,[25] all the studies addressing the photophysical properties of mono- and multifunctionalized C_{60} derivatives rely entirely on experimental results, and thus do not characterize the physical processes responsible for the observed spectral changes.

[a)]Electronic mail: rcolin@ulb.ac.be

This paper focuses on the properties of five multifunctional C_{60} derivatives ($C_{60}Cl_6$, $C_{60}Ph_5Cl$, $C_{60}Ph_5H$ and two isomers of $C_{60}Ph_5OH$) using steady-state absorption and fluorescence spectroscopy and quantum-chemical calculations. The main objective of the present analysis is to determine the effects of symmetry breaking, perturbation of the π-electronic system, and nature of the addended groups on the photophysical properties of fullerene compounds. The paper is organized as follows: first, we briefly describe the experimental and theoretical methods used in the present work. Then the optimized geometry, the related ground-state properties, and the experimental and calculated spectroscopic properties are presented for each derivative. Finally, the influence of symmetry and chemical nature of the addends/substituents on these properties is discussed.

II. EXPERIMENTAL AND THEORETICAL METHODS

A. Synthesis

The improved procedures followed to synthesize $C_{60}Cl_6$ (Ref. 32) and $C_{60}Ph_5Cl$ (Ref. 33) as well as the preparation and characterization of the $C_{60}Ph_5OH$ regioisomers will be the subject of a forthcoming manuscript.[34] $C_{60}Ph_5H$[33] was prepared as published.

B. Spectroscopic measurements

A concentrated ($\sim 10^{-4}$ mol ℓ^{-1}) and a dilute ($\sim 10^{-6}$ mol ℓ^{-1}) solution in cyclohexane were used for each derivative. Absorption spectra were recorded with a HP 8452A spectrophotometer in the 190–820 nm range, with 2 nm increments. Concentrated and dilute solutions were used to record the absorption in the visible and in the UV region, respectively. Fluorescence spectra of the concentrated solutions were recorded with a Shimadzu RF-5001PC spectrofluorophotometer. The apparatus consists of two monochromators placed at right angles, the first being equipped with a Xe lamp at the entrance slit and the other with a photomultiplier tube at the exit slit.

C. Quantum-chemical calculations

The starting geometry of the fullerene compounds were initially derived from IR and nuclear magnetic resonance spectra and then modeled at the molecular mechanics level, using the universal force field[35] parametrization; the geometry was subsequently optimized at the semiempirical Hartree–Fock Austin Model 1 (AM1) level,[36] using a ''quasi-Newton'' second derivatives method implemented in the GAUSSIAN 94 program.[37] The ground-state properties of the hexa-functionalized C_{60} derivatives were derived from the AM1 results obtained with the GAUSSIAN 94 and MOPAC 93 packages.[38] A special emphasis has been placed on the heats of formation, atomic charges, ionization potentials, and electron affinities calculated for the various derivatives. The heats of formation were evaluated following Dewar's approximation[36,39] while the net atomic charges were obtained by a Mulliken population analysis;[40] ionization potentials and electron affinities were estimated from Koopmans' approximation[41] and are therefore directly related to the calculated energies of the highest occupied molecular orbital (HOMO) and lowest unoccupied molecular orbital (LUMO) levels, respectively.

The LCAO (linear combination of atomic orbitals) coefficients that we refer to were those calculated with the semiempirical Hartree–Fock intermediate neglect of differential overlap method developed by Zerner and co-workers (INDO/S),[42] with the electron interaction terms expressed by the Mataga–Nishimoto potential.[43] These coefficients are used to quantify the localization of the molecular orbitals on the C_{60} cage according to the dimensionless *participation number* (PN). This parameter was defined in 1970 by Bell, Dean, and Hibbins-Buttler[44] to quantify the degree of localization of normal modes of vibration for atoms in a crystal lattice and was used subsequently to analyze the localization of molecular orbitals in polymer chains.[45] The PN is calculated within the INDO/S methodology as

$$\mathrm{PN}=\frac{[\Sigma_\lambda c_{i\lambda}^2]^2}{\Sigma_\lambda c_{i\lambda}^4}=\frac{1}{\Sigma_\lambda c_{i\lambda}^4}, \tag{1}$$

where $c_{i\lambda}$ is the LCAO coefficient on the λth atom in the ith molecular orbital. Using the LCAO coefficients calculated at the INDO/S level and the graphical interface INSIGHTII of molecular simulations,[46] we have also plotted the HOMO and LUMO wave functions in order to improve the visualization of their localization over the molecule.

The C_{60} derivatives studied in this work are closed-shell systems. Only the electric dipolar transitions from the ground state S_0 to the singlet excited states S_n will be considered. The excitation energies and oscillator strengths of these S_n-S_0 transitions were calculated using the INDO/S method coupled to a SCI (single configuration interaction) technique. The configurations included in the SCI development were generated from the fundamental electronic configuration associated with the AM1-optimized geometry, by promoting an electron from one of the x HOMOs to one of the y LUMOs, $(x \text{ times } y)+1$ thus defines the total size of the active space. The CI calculations performed in this work, including a maximal number of $(75\times 75)+1$ configurations, are considerably larger than most of the earlier quantum-chemical calculations reported on C_{60} (Refs. 47–58) and C_{60} derivatives.[25]

We have initially validated the INDO/SCI approach by applying it to C_{60} and C_{70}. The corresponding results are very similar to those reported by Bendale, Baker, and Zerner.[47] Indeed, comparing our results to the largest CI calculations of the latter authors reveals that the differences in the excitation energy values never exceeds 0.11 eV, whereas the oscillator strengths values for the allowed electronic transitions agree to within a factor of 2. As discussed in the paper of Bendale, Baker, and Zerner, the INDO/SCI approach appears reliable only in the energy range of less than 5 eV. The oscillator strengths calculated at higher energies are strongly underestimated with respect to the experimental data. This upper limit is expected for this all-valence-electron approach[59] and accordingly, the present analysis will be restricted to excitation energies below 5 eV for each derivative.

The excitation energies and oscillator strengths calculated for the $S_n - S_0$ electronic transitions yield a ''bar spectrum,'' which can be used to analyze the absorption spectra. However, since the number of optically allowed electronic transitions for the low symmetry C_{60} derivatives is expected to be large, it is useful to compare the experimental data to a ''synthetic'' spectrum, obtained by convoluting the ''bar spectrum'' with Gaussian functions; the full width at half-maximum (FWHM) is therefore chosen to represent a mean broadening parameter.

III. RESULTS

A. Geometry

In their stable configuration, $C_{60}Cl_6$, $C_{60}Ph_5Cl$, $C_{60}Ph_5H$ and one of the $C_{60}Ph_5OH$ isomers have their functional groups attached to the carbon atoms C(1), C(2), C(4), C(11), C(15), and C(30)[32,33] according to the numbering system recommended by IUPAC.[60] The hydrogen (chlorine) atom in $C_{60}Ph_5H$ ($C_{60}Ph_5Cl$) as well as the hydroxyl group in one of the $C_{60}Ph_5OH$ isomers (isomer 1) are attached to the cage such that the three derivatives are at first sight characterized by a plane of symmetry, as is the case for $C_{60}Cl_6$ (see Fig. 1). However, for the pentaphenylated derivatives, it has been shown experimentally[33] that the phenyl groups rotate freely at room temperature; C_s symmetry is thus only encountered in $C_{60}Cl_6$ while the configurations of $C_{60}Ph_5Cl$, $C_{60}Ph_5H$, and $C_{60}Ph_5OH$-isomer 1 can be referred to as ''pseudo-C_s symmetric.'' By contrast, the second isomer of $C_{60}Ph_5OH$ (isomer 2) where the hydroxyl group is believed to be attached to carbon atom C(9) of the cage [Fig. 1(d)] has a complete reduction in its symmetry.

The functionalization of C_{60} implies that the cage C–C double bonds are modified and that the carbon atoms to which the addends are attached undergo a transition from sp^2 to sp^3 character. The hexa-functionalization studied here significantly modulates the single versus double character of the bonds over the cage. In the symmetric and pseudosymmetric derivatives, the moiety of the cage surrounded by the functional groups is significantly modified and consists of a cyclopentadienyl entity adjacent to five hexagons each containing two 1:4 situated sp^3 carbon atoms [see for instance Fig. 1(e) for $C_{60}Ph_5H$]; the remaining part of the cage is weakly effected upon functionalization. This situation contrasts with the properties of monofunctionalized C_{60} derivatives, where all of the double bonds remain external to the pentagons.[17] It is worth noting that, in general, it is accepted that the presence of double bonds within a pentagon destabilizes fullerenes.[61–63]

The AM1-calculated bond lengths associated with the functionalized part of the cage for each derivative are reported in Table I. When compared with the parent C_{60} molecule (characterized by two bonds of 1.455 and 1.391 Å for the double and single C–C bonds, respectively[64]), the main geometric changes upon functionalization are induced by the formation of sp^3 carbon atoms; the C–C single bonds involving these sp^3 carbon atoms are longer than 1.50 Å. For the proposed structure of the asymmetric $C_{60}Ph_5OH$ isomer 2, an exceptionally long bond (1.645 Å) is calculated between the adjacent sp^3 carbon atoms C(1) and C(9) bearing a phenyl and the hydroxyl group, respectively; a third double bond in a pentagon [between C(10) and C(11)] is observed in this compound. The bond lengths calculated for the symmetrical $C_{60}Ph_5OH$ isomer 1 are in good agreement (maximal deviation below 0.03 Å) with respect to the experimental values provided by x-ray diffraction measurements.

The cage bond lengths are very similar among the 1,2,4,11,15,30-hexafunctionalized C_{60} derivatives. We note however that: (i) most of the single C–C bonds involving an sp^3 carbon in $C_{60}Cl_6$ are smaller by some 0.006 Å than those in the other derivatives; and (ii) the **i** and **j** bonds involving the C(2) carbon atom are longer for $C_{60}Ph_5OH$ (1.561 and 1.548 Å) than for $C_{60}Ph_5Cl$ (1.551 and 1.539 Å) and markedly larger than those of $C_{60}Ph_5H$ (1.540 and 1.527 Å). Although these variations are not larger than the mean deviations between the theoretical and experimental data obtained for $C_{60}Ph_5OH$, the calculations clearly show that only the bonds involving C(2) (i.e., **i** and **j** bonds in Table I) significantly differ among the derivatives. This suggests that these two bonds are the most sensitive to addend and/or steric effects, as discussed in more detail in the following.

B. Ground-state electronic properties

The AM1-calculated heats of formation of the various compounds are given in Table II. Taking into account the fact that these values for C_{60} and C_{70} are overestimated by about 300 kcal mol^{-1} with respect to the experimental data,[65] the values reported in Table II should be considered with caution. We also note that a detailed comparison between the values obtained for the derivatives may be affected by the changes in the nature of the functional group. However, the difference between the calculated heats of formation of the two $C_{60}Ph_5OH$ isomers is expected to be reliable; this suggests a higher stability for the pseudosymmetric isomer 1 ($\Delta H_f = 981$ kcal mol^{-1}) with respect to its asymmetric homolog ($\Delta H_f = 1007$ kcal mol^{-1}), as expected from the geometry considerations.

We have also analyzed by means of the Mulliken population analysis the electron-donating or electron-withdrawing character of the addended/substituted groups and the way that the transferred charges are distributed among the carbon atoms of the cage; the results are collected in Table II. The functional groups in total possess a global donor character in the C_{60} derivatives considered, the exception being $C_{60}Cl_6$ in which the chlorine atoms remain almost neutral with respect to the cage (the overall contribution is $-0.003\ |e|$). The phenyl groups have a weak electron-donating character in all cases ($+0.03 \pm 0.02\ |e|$ typically donated to the cage per phenyl group). The chlorine atom in $C_{60}Ph_5Cl$ and the hydroxyl group in both isomers of $C_{60}Ph_5OH$ have a weak acceptor character and reduce the dominant electron-donating character of the phenyl groups; the electron donation is increased in $C_{60}Ph_5H$, where the hydrogen atom operates as a stronger donor ($+0.217\ |e|$) than the phenyl groups.

In all of the derivatives, the functional groups lead to a distribution of the donated charges toward that part of the cage opposite to the functionalized area (referred to as the ''unmodified part'' in Table II). This effect is most pro-

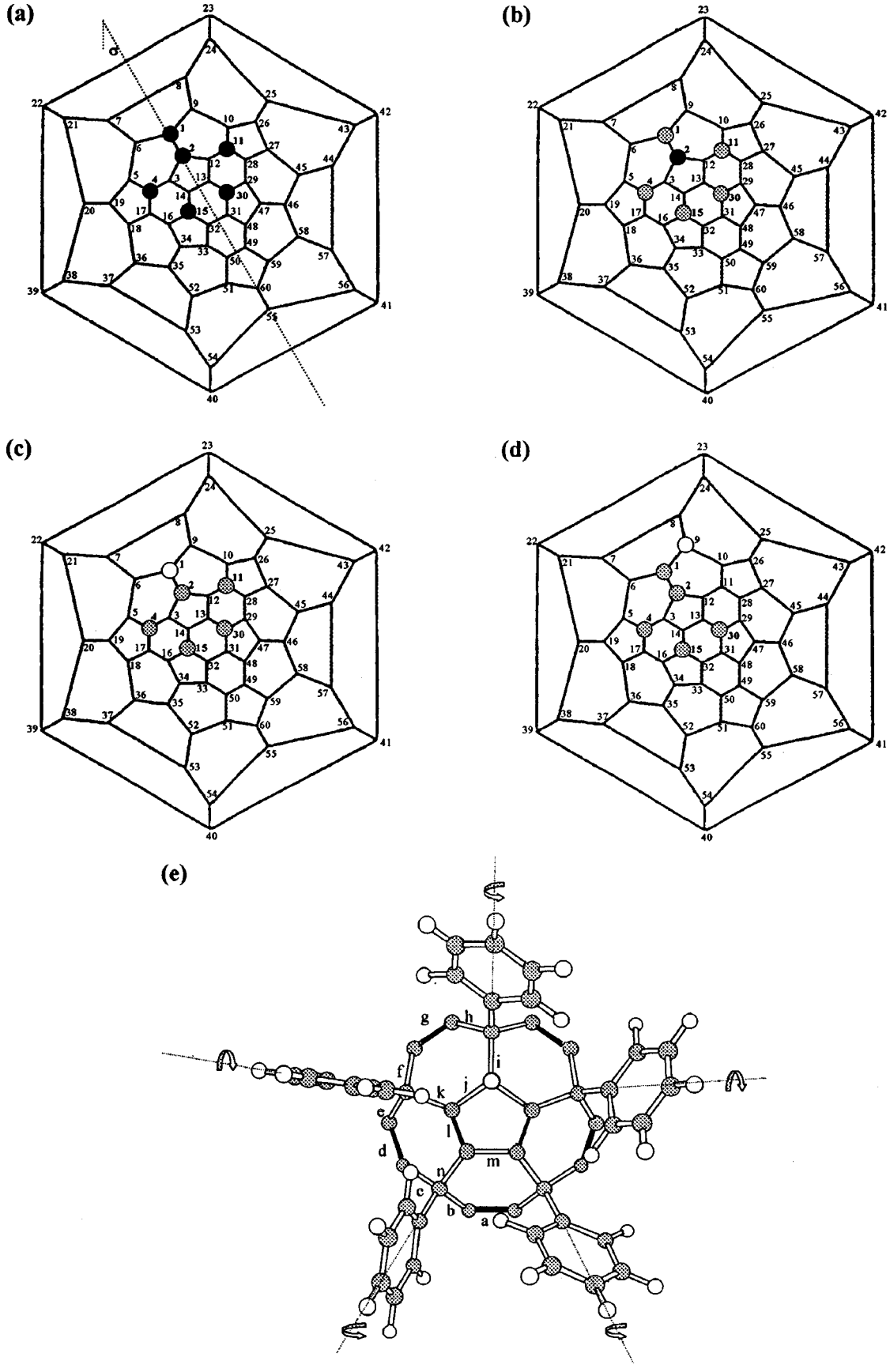

FIG. 1. Schlegel diagrams of: (a) $C_{60}Cl_6$, (b) $C_{60}Ph_5Cl$, and $C_{60}Ph_5H$, (c) $C_{60}Ph_5OH$-isomer 1, and (d) $C_{60}Ph_5OH$-isomer 2. The black balls represent the chlorine atoms [or the hydrogen atom in (b)], the gray balls refer to the phenyl groups, and the white balls to the hydroxyl group. The IUPAC numbering system is adopted (Ref. 60). The functionalized part of $C_{60}Ph_5H$ provided by the AM1 calculations is given in (e); in this figure, the gray and white balls correspond to carbon and hydrogen atoms, respectively, while the thick black lines represent double bonds.

TABLE I. AM1-calculated bond lengths (in angstrom) in the functionalized part of the C_{60} derivatives. The bond labeling refers to that given in Fig. 1(e). We also report in parentheses the experimental bond lengths in $C_{60}Ph_5OH$ provided by x-ray diffraction experiments (Ref. 34).

	$C_{60}Cl_6$	$C_{60}Ph_5Cl$	$C_{60}Ph_5H$	$C_{60}Ph_5OH$ isomer 1	$C_{60}Ph_5OH$ isomer 2
a	1.368	1.368	1.368	1.366 (1.369)	1.367
b	1.530	1.536	1.537	1.536 (1.550)	1.539
c	1.532	1.538	1.540	1.538 (1.542)	1.535
d	1.368	1.368	1.369	1.367 (1.358)	1.366
e	1.539	1.546	1.545	1.546 (1.544)	1.547
f	1.527	1.534	1.536	1.533 (1.543)	1.532
g	1.364	1.364	1.366	1.368 (1.364)	1.368
h	1.529	1.535	1.532	1.537 (1.530)	1.522
i	1.547	1.551	1.540	1.561 (1.581)	1.572
j	1.539	1.539	1.527	1.548 (1.556)	1.558
k	1.490	1.497	1.496	1.501 (1.511)	1.498
l	1.367	1.368	1.370	1.368 (1.339)	1.373
m	1.472	1.476	1.472	1.475 (1.471)	1.469
n	1.493	1.501	1.499	1.500 (1.523)	1.502
h'					1.645

nounced for the asymmetric $C_{60}Ph_5OH$ (isomer 2) and is very weak for $C_{60}Cl_6$. The latter result confirms the small electron donation from the cage to the chlorine atoms. Both the functionalized and unmodified parts of the cage in $C_{60}Ph_5Cl$ and $C_{60}Ph_5H$ (where the global electron-donating character of the functional groups is strongest) have an excess charge. In contrast, the functionalized part of the cage also acts as an electron donor in the case of the $C_{60}Ph_5OH$ isomers.

The graphical representations of the HOMO and LUMO orbitals of each derivative are shown in Fig. 2 together with the corresponding participation number (PN) calculated using Eq. (1). Figure 2 clearly illustrates that the functional groups weakly contribute to the molecular orbital description of the frontier levels provided that the C_s or pseudo-C_s symmetry is preserved. This is particularly true for the HOMO orbitals of the symmetrical and pseudosymmetrical hexa-functionalized derivatives, which are mostly localized on the equatorial belt (in agreement with earlier theoretical results reported for $C_{60}Ph_5K$ complexes[66]) and are characterized by a very similar participation number: 42.2 ± 0.5. The LUMO levels of these derivatives are also localized on the unmodified part of the C_{60} cage but present larger fluctuations in the PN (varying from 44.6 to 58.1). The reduction in symmetry in going from the pseudo-C_s symmetrical $C_{60}Ph_5OH$ (isomer 1) to the asymmetric isomer 2, significantly modifies the characteristics of both the HOMO and LUMO orbitals. This is illustrated by the fact that the frontier orbitals of the asymmetric $C_{60}Ph_5OH$ gain significant weight on the carbon atoms forming the ''functionalized part'' of the cage, where the HOMO level is mostly localized (with a PN of only 22.1).

The ionization potential (I) and electron affinity (A) evaluated with Koopmans' approximation, correspond in absolute value to the Hartree–Fock energy of the HOMO and LUMO levels, respectively. The difference (I-A) represents the HOMO–LUMO gap (ΔE), which is a useful parameter when analyzing the spectroscopic properties of the fullerence derivatives, as shown later. The values of I, A, and ΔE calculated at the semiempirical AM1 and INDO/S level for each derivative are collected in Table II. The comparison between the calculated values and the experimental data reported for C_{60} in the gas phase ($I = 7.61 \pm 0.02$ eV[67] and $A = 2.65 \pm 0.05$ eV[68]) indicates that the INDO/S method yields a somewhat more accurate estimate of the first ionization potential although it does not reproduce the value of the electron affinity as well as the AM1 method. The shifts in the HOMO and LUMO levels energies provided by the two approaches are very similar when going from one functionalized derivative to the others; a detailed analysis reveals, however, that the balance between the σ-acceptor inductive vs π-donor mesomer characters is subject to variations between the INDO/S and AM1 parametrizations, despite the fact that

TABLE II. Ground-state properties (heat of formation ΔH_f, charge distribution, ionization potential I, electron affinity A, and HOMO–LUMO gap ΔE) of the C_{60} derivatives, as calculated at the AM1 level. We provide the total Mulliken net charges supported by the functional groups as well as by the ''functionalized'' (summed over 20 carbon atoms) and ''unmodified'' (summed over 40 carbon atoms) parts of the molecule. The INDO/S values calculated for I, A, and ΔE are also given in parentheses.

	C_{60}	$C_{60}Cl_6$	$C_{60}Ph_5Cl$	$C_{60}Ph_5H$	$C_{60}Ph_5OH$ isomer 1	$C_{60}Ph_5OH$ isomer 2
ΔH_f(kcal×mol^{-1})	974	847	1016	1010	981	1007
Charge distribution ($\|e\|$)		−0.007/Cl on C(1)	+0.044/Ph on C(1)	+0.019/Ph on C(1)	−0.070/OH on C(1)	+0.010/Ph on C(1)
		+0.006/Cl on C(2)	−0.044/Cl on C(2)	+0.217/H on C(2)	+0.029/Ph on C(2)	+0.028/Ph on C(2)
		−0.001/Cl on C(4)	+0.036/Ph on C(4)	+0.028/Ph on C(4)	+0.037/Ph on C(4)	+0.031/Ph on C(4)
		−0.001/Cl on C(11)	+0.040/Ph on C(11)	+0.030/Ph on C(11)	+0.031/Ph on C(11)	−0.064/OH on C(9)
		0.000/Cl on C(15)	+0.040/Ph on C(15)	+0.033/Ph on C(15)	+0.033/Ph on C(15)	+0.035/Ph on C(15)
		0.000/Cl on C(30)	+0.034/Ph on C(30)	+0.033/Ph on C(30)	+0.030/Ph on C(30)	+0.038/Ph on C(30)
Functional groups (total)		−0.003	+0.150	+0.359	+0.089	+0.078
Functionalized part		+0.016	−0.007	−0.183	+0.051	+0.152
Unmodified part		−0.013	−0.143	−0.176	−0.140	−0.230
I (eV)	9.64 (6.63)	9.63 (7.14)	9.09 (6.63)	9.01 (6.47)	9.06 (6.51)	8.81 (6.20)
A (eV)	2.98 (1.07)	2.80 (1.43)	2.29 (0.85)	2.22 (0.75)	2.27 (0.81)	2.50 (1.09)
ΔE (eV)	6.66 (5.56)	6.83 (5.71)	6.80 (5.78)	6.79 (5.72)	6.79 (5.70)	6.31 (5.11)

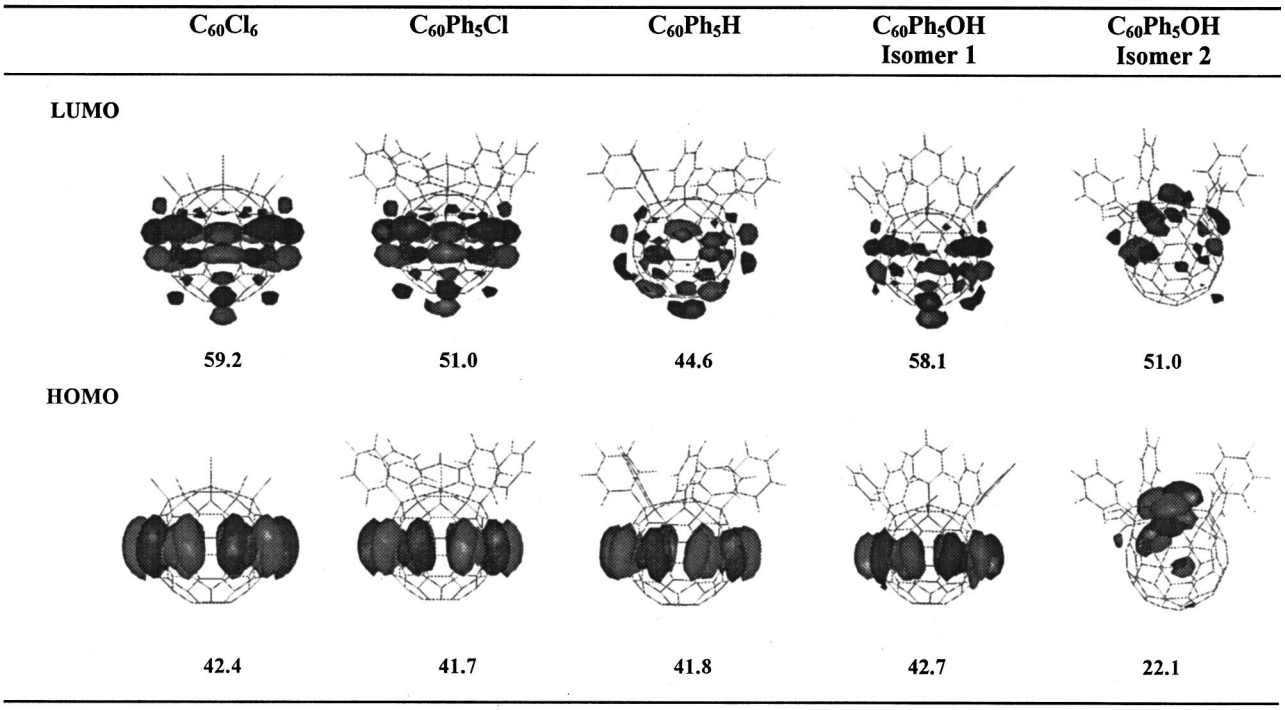

FIG. 2. Graphical representation of the HOMO and LUMO wave functions based on the INDO/S-calculated LCAO coefficients; the participation number PN is given below each orbital.

the global effect on I and A is very similar. Both methods may thus be used for our study whose primary goal is to compare the relative evolution of the calculated properties among the various derivatives. It must be stressed that the calculated evolution of I and A going from C_{60} to any functionalized derivative under study is strongly dependent on the method used. We have chosen to discuss in the following the results provided by the AM1 calculations that better match the corresponding shifts calculated at the *ab initio* Hartree–Fock 6-31G* level (stabilization by 0.25 eV of the HOMO level and destabilization of 0.07 eV of the LUMO level when going from C_{60} to $C_{60}Cl_6$).

The energetic diagram, Fig. 3, shows the AM1-calculated energies of the HOMO and LUMO levels in C_{60} and its derivatives and offers an improved illustration of the evolution of the frontier levels of the cage upon functionalization. The AM1 results show that the hexa-functionalization of the C_{60} cage systematically destabilizes the HOMO and LUMO levels. For the symmetrical and pseudosymmetrical derivatives, it appears that the destabilization of the frontier molecular orbitals correlates with the increasing strength of the global electron-donating character of the addended/substituted groups (i.e., the largest destabilization is obtained for $C_{60}Ph_5H$ in which the largest global charge transfer takes place between the cage and the substituents). The HOMO–LUMO gap ΔE in $C_{60}Cl_6$ and the pseudosymmetrical derivatives are very similar (values of 6.81 ± 0.02 eV and 5.74 ± 0.04 eV calculated at the AM1 and INDO/S level, respectively) due to the fact that the asymmetry in the destabilization of the HOMO and LUMO levels with respect to C_{60} is almost identical in the various compounds. In contrast, the asymmetric isomer of $C_{60}Ph_5OH$ is characterized, with respect to the other functionalized cages, by a considerably lower ionization potential; the destabilization of the HOMO level is much larger than that of the LUMO for this derivative and thus leads to a weaker value for the HOMO–LUMO gap ΔE (6.31 and 5.11 eV according to the AM1 and INDO/S results, respectively). It must be emphasized that the destabilization of the HOMO level in the asymmetric isomer of $C_{60}Ph_5OH$ may be related to its strong localization on the cage (associated with a small value of PN), as discussed in a forthcoming paper.[69]

C. Spectroscopic properties

The absorption and fluorescence spectra of each of the derivatives dissolved in cyclohexane are shown in Fig. 4. The intensity of the absorption spectra is reflected by the extinction coefficients, which are, however, subject to large errors due to the small quantities of samples available. In accordance with Kasha's rule, the fluorescence spectrum does not change with the excitation wavelength, thus providing good evidence that the observed bands correspond to the $S_1 \rightarrow S_0$ electronic transition. The wavelengths associated with the maximum of the main absorption features and fluorescence band (together with other photophysical quantities discussed below) are collected in Table III and these values are compared with those obtained for C_{60} under similar experimental conditions.

$C_{60}Ph_5Cl$, $C_{60}Ph_5H$, and the pseudosymmetric $C_{60}Ph_5OH$ isomer 1 have similar spectroscopic properties. Their absorption spectra in the UV and visible range display nine features, labeled *a* to *i* in Fig. 4. The absorption spectrum of $C_{60}Cl_6$ is noteworthy as it is less resolved so that bands *a*, *c*, *e* and *f* cannot be distinguished. The UV absorption features (bands *h* and *i*) of the C_s and pseudo-C_s sym-

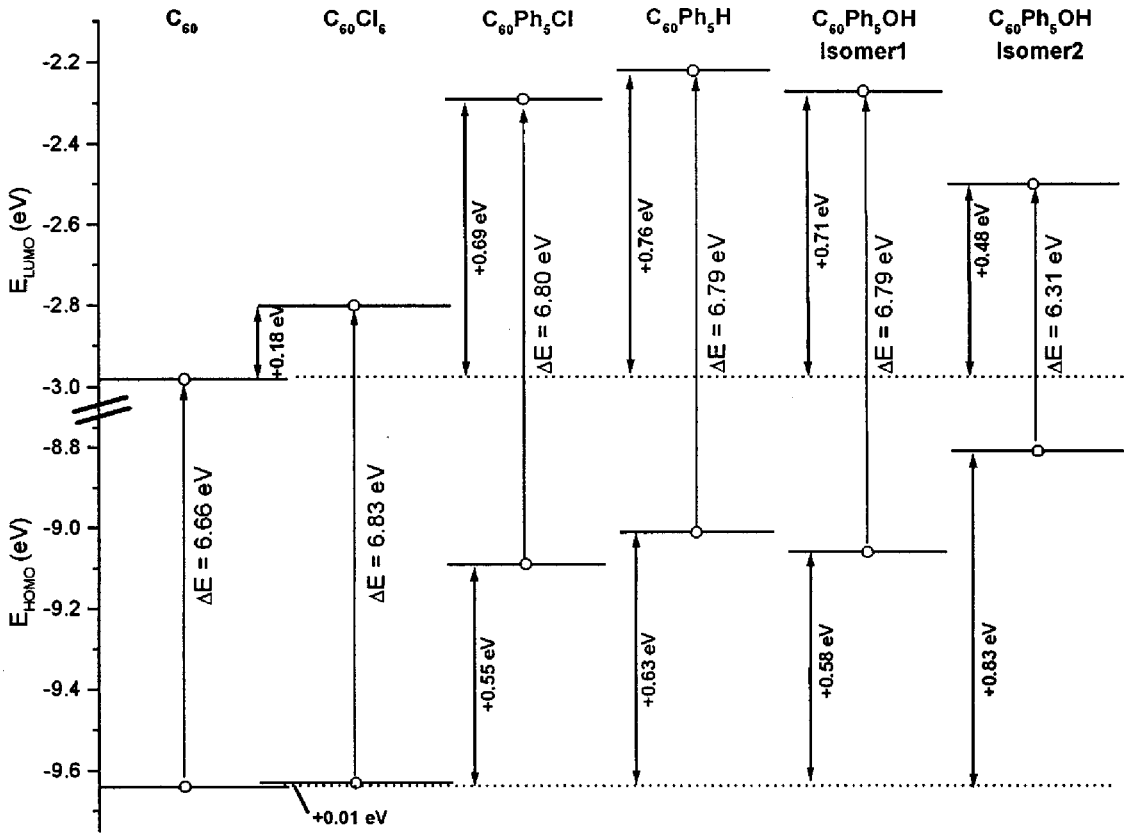

FIG. 3. Energy diagram illustrating the AM1-calculated energies of the HOMO and LUMO levels of C_{60} and hexa-functionalized derivatives under study. The dashed lines represent the energy reference given by the frontier orbitals of C_{60}. The values of the HOMO–LUMO gap (ΔE) and the shifts of the HOMO and LUMO levels with respect to C_{60} are also reported.

metrical derivatives are very close in energy to those observed for C_{60}. They are however much broader and have a weaker absolute intensity (hypochromic effect) as a result of the loss of icosahedral symmetry [see for instance the spectrum of $C_{60}Ph_5H$ in Fig. 5(a)]. By contrast, the visible part of the spectra of the functionalized derivatives differ markedly from that of C_{60}. In particular, the absorption is more intense down to wavelengths of 500 nm and drops sharply to zero at longer wavelengths. The fluorescence spectra of the derivatives, which consist of a single broad band peaking at 624 ± 5 nm, are blueshifted, as is the onset of absorption, with respect to C_{60}. The fluorescence band is shifted by some 150 nm from the lowest resolved absorption band *b* and does not show a mirror image of the absorption line shape. Accordingly, the energy of the S_1 state is estimated as being equal to the energy at the intersection between the fluorescence and absorption spectra. This procedure yields a value of 2.24 ± 0.5 eV for each symmetrical and pseudosymmetrical derivative despite the inaccuracy of the method (Table III).

The INDO/SCI-calculated ''bar'' and ''synthetic'' spectra provide further insight into the spectroscopic properties of the hexa-functionalized C_{60} derivatives under study. The spectra are discussed on the basis of the results obtained with the largest CI active space (containing up to 5625 singly excited configurations). It is expected that the calculated values will converge by increasing the size of the active space, and also come closer to the measured values. This effect is rather small for the first vertical excitation energy values (0.02 eV when going from 1600 to 5625 excited configurations); it becomes more significant when considering higher energy transitions. It is also observed that the oscillator strengths values vary little with the size of the active space (less than 20% for transitions below 4 eV). For each derivative, the INDO/SCI simulations are in very good agreement with the experimental spectrum and allow for a detailed assignment of the absorption features. For clarity, the bar and synthetic spectra calculated for $C_{60}Ph_5H$ together with the corresponding experimental spectrum are plotted in Fig. 5(b). The calculated spectrum has been normalized with respect to the intensity of the experimental band *h* and rigidly redshifted by 1200 cm^{-1} to improve the fit between theory and experiment; this shift can be attributed to intermolecular polarization effects neglected in our calculations. FWHM values of 0.3 eV are used to simulate the spectra in the visible and UV regions. It should also be noted that the calculated oscillator strengths agree within a factor of 3 with those measured, assuming a Gaussian profile for the observed bands, in the low energy part of the absorption spectrum (bands $a-d$). At higher energies, this comparison becomes difficult due to the strong congestion of the spectrum in that region. From Fig. 5(b), it is obvious that the calculated spectra match the experimental data very well over the whole spectral range. This is particularly the case in the visible range where the bands $a-d$ can be unambiguously assigned

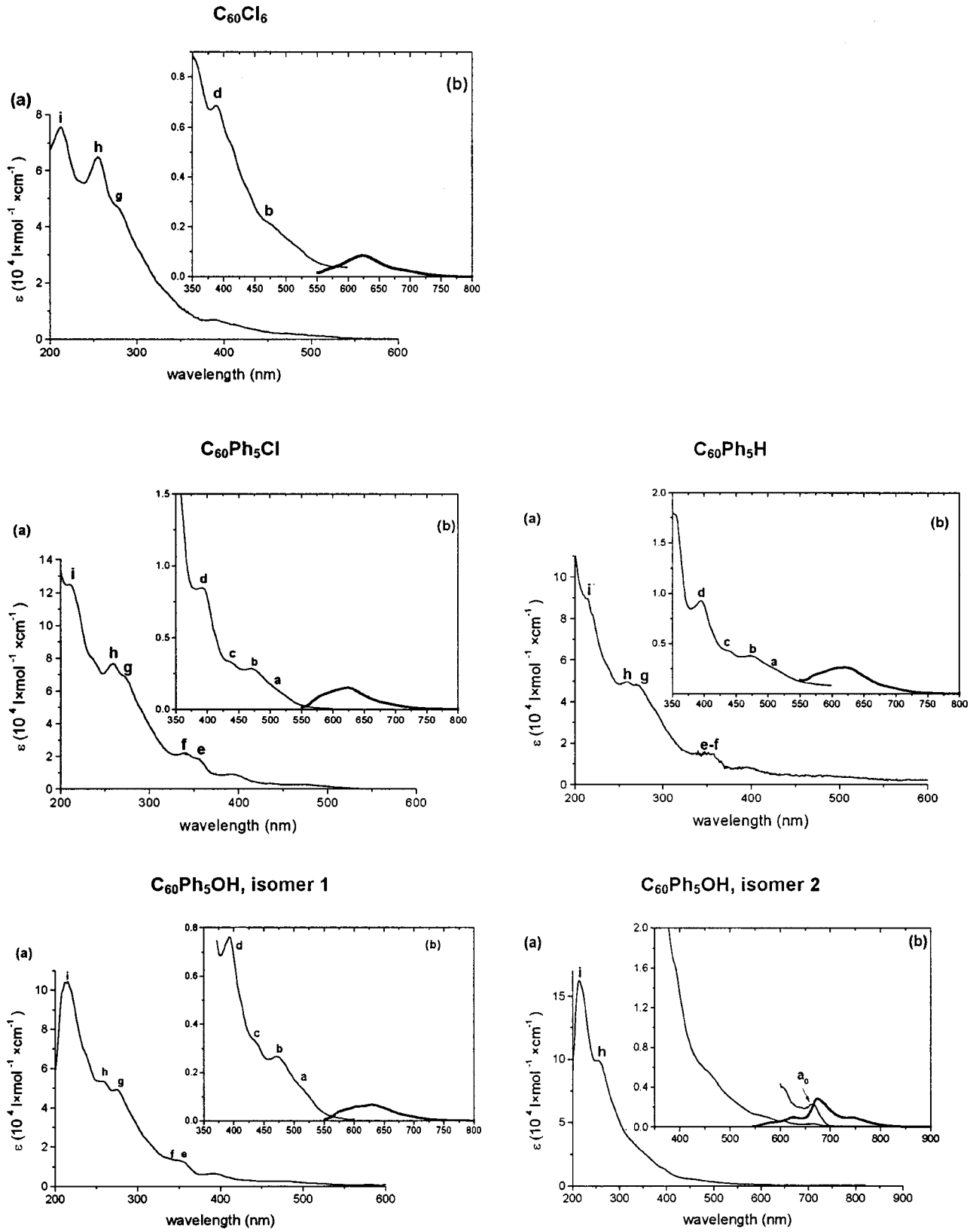

FIG. 4. Experimental UV–visible absorption (thin line) and fluorescence (thick line) spectra of the C_{60} derivatives dissolved in cyclohexane. The inset window displays for each derivative the fluorescence spectrum expressed in arbitrary units together with the lowest absorption features in the absorption spectrum.

to one or a set of electronic transitions; in turn, each transition can be associated with a one-electron excitation between a given occupied and unoccupied molecular orbital. Such an analysis is reported for $C_{60}Ph_5H$ in Table IV. In view of their spectral similarities (see Table III), the optical features observed in the absorption spectra of $C_{60}Cl_6$, $C_{60}Ph_5Cl$, and $C_{60}Ph_5OH$-isomer 1 are assigned in a similar way. The foregoing data therefore lead to the following conclusions re-

TABLE III. Photophysical properties collected for C_{60} and the hexa-functionalized derivatives; the band labeling refers to that given in Fig. 4.

	$C_{60}Cl_6$	$C_{60}Ph_5Cl$	$C_{60}Ph_5H$	$C_{60}Ph_5OH$ isomer 1	$C_{60}Ph_5OH$ Isomer 2	C_{60}[a]
Absorption bands (λ, nm)						
i	213	209	214	214	214	214 (*G*)
						230 (*F*)
h	255	259	259	258	256	258 (*E*)
g	274	272	270	274		294 (*D*)
f		339	340	334		330 (*C*)
e		351	351	348		378 (B_0)
d	388	394	394	392	388	392(A_3) 404 (A_0-A_1)
c		438	435	432	445	422 (ζ)
b	470	474	475	472		
a		516	515	510		
						504-620 ($\gamma-\epsilon$)
a_0					666	
Fluorescence band (λ, nm)	624	624	622	629	675 742	688 718
Excitation energy S_0-S_1 (eV)						
Measured	2.25	2.25	2.29	2.19	1.85	1.95[b]
Calculated	2.45	2.45	2.46	2.45	1.96	2.32
S_1 lifetime (ns)	0.5	1.2	1.2			1.17[c]

[a]The band notation for C_{60} is that proposed by Leach *et al.* (Ref. 75).
[b]Following Sassara, Zerza, and Chergui (Ref. 72).
[c]Following Kim for C_{60} in toluene (Ref. 76).

garding the optical properties of the C_s and pseudo-C_s symmetrical hexa-functionalized derivatives examined.

(1) The first dominant absorption band *b* originates from the superposition of three optical transitions between S_0 and the seventh, eighth, and ninth excited states; the weak shoulder *a* is attributed to the $S_0 \rightarrow S_2$ electronic transition.

(2) The electronic transition from S_0 to the first excited state S_1 is calculated at 2.45 ± 0.1 eV and displays a vanishingly small oscillator strength. The very weak intensity of this transition rationalizes the reason whereby the lowest excited state cannot be located in the absorption spectrum and is detected only through its weak fluorescence signal. The calculated S_0-S_1 excitation energy is in very good agreement with the value of 2.24 ± 0.5 eV estimated from the absorption and fluorescence spectra; the matching is further improved when considering the systematic redshift of 1200 cm^{-1} adopted to simulate the spectra of the derivatives. The calculations also indicate that the 1,2,4,11,15,30-

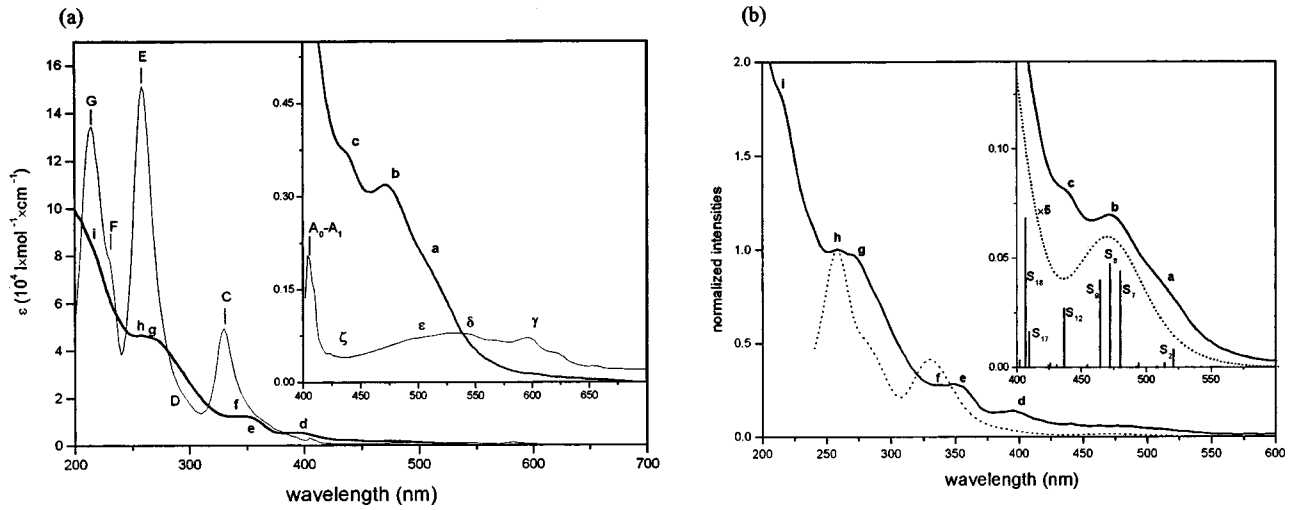

FIG. 5. (a) Experimental UV–visible absorption spectra of $C_{60}Ph_5H$ in cyclohexane (thick line) and of C_{60} in similar conditions, given as a reference (thin line); (b) measured (solid line) and calculated ''synthetic'' (dotted line) absorption spectra of $C_{60}Ph_5H$. The calculated ''bar'' spectrum is also shown in the visible region, where the most intense electronic transitions are assigned to the corresponding excited states S_n. The calculated spectrum is rigidly redshifted by 1200 cm^{-1} and normalized to the intensity of the experimental band *h*.

TABLE IV. Wavelengths associated with the maximum of the measured and calculated ''synthetic'' absorption bands in $C_{60}Ph_5H$ (the theoretical values refer to the synthetic spectrum rigidly redshifted by 1200 cm^{-1}). The bands observed in the experimental spectra are assigned to calculated optically allowed electronic transitions [Fig. 5(b)] whose main CI configuration is given in the last column.

	Experimental λ (nm)	Calculated λ (nm)	Electronic transitions	Dominating electronic excitations
a	515	523	$S_2 \leftarrow S_0$	[LUMO+2←HOMO]
			$S_3 \leftarrow S_0$	[LUMO←HOMO−1]
b	475	473	$S_7 \leftarrow S_0$	[LUMO+3←HOMO]
			$S_8 \leftarrow S_0$	[LUMO←HOMO−1]
			$S_9 \leftarrow S_0$	[LUMO←HOMO−2]
c	435	437	$S_{12} \leftarrow S_0$	[LUMO+2←HOMO−2]
d	394	401	$S_{17} \leftarrow S_0$	[LUMO+4←HOMO−1]
			$S_{18} \rightarrow S_0$	[LUMO+2←HOMO−3]
e	351			
f	340	329		
g	270			
h	259	258		
i	214			

hexafunctionalization of the C_{60} cage induces a hypsochromic shift of the lowest excited state (the S_0-S_1 transition is calculated to be 2.32 eV in C_{60}).

(3) The absorption bands in the visible part of the spectrum can be assigned to specific electronic transitions which in most cases can be described by a one-electron excitation between an occupied and unoccupied orbitals localized on the unmodified part of the cage. The assignment of the optical bands in the UV region is much more complex due to the high density of electronic transitions in this energy range. Some of the high-energy transitions give rise to a photoinduced electron transfer from the cage to the substituent phenyl groups, as discussed in a previous publication.[70]

The spectroscopic properties of the asymmetric isomer 2 of $C_{60}Ph_5OH$ significantly differ from those of the pseudosymmetrical homolog and related 1,2,4,11,15,30-hexafunctionalized derivatives. The asymmetric molecule is characterized by broader absorption bands in the UV and the visible regions, where the bands $a-b$ and $e-g$ can hardly be distinguished (Fig. 4). The lowest wavelength absorption feature of the asymmetric molecule (labeled a_0 in Fig. 4) is centered around 666 nm and is strongly redshifted with respect to the other derivatives. The fluorescence spectrum consisting of a main signal at 675 nm and a shoulder at 742 nm, is also shifted to a longer wavelength and mirrors the absorption band at 666 nm.[71] The energy of the S_1 excited state is estimated to be 1.85 eV by averaging the energy at the maximum of the lowest absorption and fluorescence bands; this is 0.4 eV lower than that of the symmetrical and pseudosymmetrical derivatives and 0.1 eV lower than in C_{60}.[72] The experimental findings are supported by the INDO/SCI calculations performed on the asymmetric isomer 2 which yield a lowest transition energy at 1.96 eV; the latter is redshifted with respect to the other derivatives and bears a significant oscillator strength of 0.03. The S_0-S_1 transition is mainly described by the promotion of an electron from the HOMO to the LUMO levels.

IV. DISCUSSION

The foregoing results demonstrate that the reduction of symmetry upon hexa-functionalization of the icosahedral C_{60} cage induces major changes in the optical properties with respect to the parent molecule. These changes are mainly characterized by: (1) a broadening of the absorption bands in the UV and visible regions, with a marked hypochromic effect in the UV; and (2) major changes of the low energy part of the spectrum, which gives rise to the absorption in the visible region and to the fluorescence signal. The greater reduction of symmetry taking place in going from the pseudo-C_s symmetric (isomer 1) to the asymmetric $C_{60}Ph_5OH$ isomer 2 leads to similar effects. Indeed, when the absorption spectrum of the asymmetric derivative is compared with that of the pseudosymmetric isomer 1 significant changes in the excitation energies and related intensities in the visible region, in addition to broader optical features in both the UV and visible range, are observed. The larger extinction coefficient measured for the asymmetric molecule is therefore unexpected.

These considerations suggest that the seemingly large broadening of the optical features in the absorption spectrum of $C_{60}Cl_6$ may not reflect the intrinsic electronic properties of the isolated molecule. This is supported by the INDO/SCI calculations, which indicate that the number of optically allowed electronic transitions in $C_{60}Cl_6$ (the only C_s-symmetrical molecule studied) is lower than that of the pseudosymmetrical phenylated derivatives. Aggregation mechanisms, which are known to significantly modify the absorption properties of fullerene related materials,[4,28,73] might result in the broadening of the absorption bands observed in the spectrum of $C_{60}Cl_6$.

The results presented clearly demonstrate that the understanding of the photophysical properties of fullerene derivatives necessitate a detailed analysis of their electronic properties. Indeed, although it is generally accepted that a reduction in the degree of symmetry induced by a functionalization of the C_{60} cage initiates a bathochromic (red) shift of the lowest absorption and fluorescence bands,[4] both the present experimental and theoretical data demonstrate that the reduction from the icosahedral symmetry of C_{60} to the C_s symmetry of 1,2,4,11,15,30-hexafunctionalized C_{60} derivatives induces a hypsochromic (blue) shift. In contrast, the loss of the C_s symmetry results, for the asymmetric $C_{60}Ph_5OH$ isomer, in a redshift of both the lowest absorption and fluorescence signals. The rationalization of the spectral properties of fullerene derivatives should thus rely not only on symmetry considerations but also on more subtle effects associated, for instance, with the degree of conjugation around the cage and the localization of the molecular orbitals. Similarly, in the recent publication of Schick *et al.*[30] the photophysical properties of hexapyrrolidino-C_{60} derivatives with T_d and D_{3h} symmetry were found to be characterized by a blueshifted absorption system (compared with C_{60}) and by a strong luminescence in the visible region. The authors suggest that these remarkable photophysical properties can be explained, to some extent, by the degree of conjugation on the C_{60} cage. In a forthcoming paper detailing the spectroscopic properties of multiply phenylated C_{70} derivatives,

an analysis of the existing relationship between conjugation effects and photophysical properties in fullerene derivatives will be presented.[69]

Both the spectroscopic and quantum-chemical investigations performed on $C_{60}Cl_6$, $C_{60}Ph_5Cl$, $C_{60}Ph_5H$, and pseudo-symmetric $C_{60}Ph_5OH$ isomer 1 indicate that the nature of the addends/substituents have a negligible influence on the electronic transition energies; it is worth noting that these derivatives are all characterized by a similar distortion of the cage geometry upon functionalization. The weak variations in the measured absorption and fluorescence band positions (see Table III) do not appear to be systematic or explainable in terms of the electron-withdrawing or electron-donating character of the addended/substituted groups. These conclusions agree with those made by other groups[7,23] but contrast with the work of Luo *et al.*,[11] which shows evidence of hypsochromic and bathochromic effects in *N*-methylpyrrolidinofullerenes depending upon the electron-withdrawing or donating character of the addends. Despite the fact that the spectroscopic properties of the derivatives under study are weakly effected by the nature of the addends/substituents, the calculations do, however, reveal that one-electron properties, such as the ionization potential (I) and electron affinity (A), can be significantly modified when going from one compound to the next. It is therefore of great interest to validate the calculated evolutions of these quantities by means of experimental measurements, probing, for example, the changes in the redox potential among the C_{60} derivatives.[74] The destabilization of the frontier levels in the symmetrical and pseudosymmetrical derivatives can be correlated to the global electron-donating character of the six addends/substituents; this correlation is further validated by the similar evolution of I and A among the functionalized derivatives calculated at both the AM1 and INDO/S levels (see Table II). The localization of the HOMO and LUMO wave functions (quantified here by the PN) can also play a role in determining the values of I and A in fullerene derivatives, as will be shown in a forthcoming paper. The PNs calculated for $C_{60}Cl_6$, $C_{60}Ph_5Cl$, $C_{60}Ph_5H$, and $C_{60}Ph_5OH$-isomer 1 show significant variations for the LUMO levels and are very similar for the HOMO levels. This leads to the conclusion that the degree of localization of the molecular orbitals is not the key parameter governing the evolution of I and A among these derivatives; this behavior is actually mostly driven by addend/substituent effects. The almost parallel evolution of I and A gives rise to an almost constant value for the HOMO–LUMO gap, thus rationalizing the weak influence of the addend/substituent on the spectroscopic properties of the C_{60} derivatives under study.

The AM1 calculations also show that the substitution of five chlorine atoms in $C_{60}Cl_6$ by phenyl groups induces an elongation (by 0.006 Å) of all of the single C–C bonds on the functionalized part of the C_{60} cage (see Table I). It is not possible to determine whether this effect is related to the electron-donating character of the phenyl groups or steric effects induced by their bulkiness. The subsequent replacement of the chlorine atom by a hydrogen atom induces a significant reduction in the length (by 0.011 Å) of the C–C bonds involving the substituted carbon atom C(2) [i.e., bonds i and j in Fig. 1(e)]. The changes are likely to be driven by the combination of an increase in the electron density around the C(2) carbon atom expected from the stronger electron-donating character of the hydrogen atom and steric effects due to the introduction of the hydrogen atom. The further increase in the length of the i and j bonds on going from $C_{60}Ph_5Cl$ to $C_{60}Ph_5OH$-isomer 1 can also be rationalized by both charge distribution and steric effects.

Preliminary results have also shown that the chemical nature of the addends/substituent modulates the fluorescence lifetime.[27] The value measured by using the ''time correlated single photon counting'' method is weaker for $C_{60}Cl_6$ (0.5 ns) than for $C_{60}Ph_5Cl$ and $C_{60}Ph_5H$ (1.2 ns). Assuming that the radiative lifetime of the compounds does not change, this effect is most probably attributable to the fact that the heavy chlorine atoms favor intersystem crossing between the first excited singlet state S_1 and the first excited triplet state T_1.

V. CONCLUSIONS

The equilibrium geometry of C_{60} derivatives ($C_{60}Cl_6$, $C_{60}Ph_5Cl$, $C_{60}Ph_5H$, and two isomers of $C_{60}Ph_5OH$) and the related ground-state properties such as heat of formation, ionization potential and electron affinity, and charge distribution have been characterized. In addition the photophysical properties of these compounds have been investigated by means of spectroscopic measurements and quantum-chemical calculations. The theoretical results indicate that the electron-withdrawing or electron-donating character of the addended/substituted groups has a small influence on the nuclear geometry, negligible effect on the spectroscopic properties, but leads to a significant change in the ionization potentials and electron affinities. The absorption and fluorescence spectra have been described in terms of optically allowed and forbidden electronic transitions and are shown to be strongly affected by the functionalization of the cage. In particular, we have demonstrated that the breaking of the icosahedral symmetry induces a broadening of the absorption bands in both the UV and visible regions; this also leads to major modifications in the fluorescence spectrum and in the low energy region of the absorption spectrum characteristic of the parent C_{60} molecule. The fluorescence signals and the lowest absorption bands are blueshifted with respect to C_{60} in the case of C_s or pseudo-C_s symmetrical derivatives ($C_{60}Cl_6$, $C_{60}Ph_5Cl$, $C_{60}Ph_5H$ and one of the $C_{60}Ph_5OH$ isomers) while a redshift prevails for the asymmetric $C_{60}Ph_5OH$ isomer. The symmetry considerations do not fully account for the observed bathochromic or hypsochromic shifts; additional work is therefore required in order to improve the understanding of the nature of the molecular and electronic properties governing the spectroscopy of functionalized fullerenes. This will be the focus of a forthcoming paper addressing the ground-state and photophysical properties of multiply phenylated derivatives of C_{70} ($C_{70}Ph_{2n}$, with $n=1-5$).

ACKNOWLEDGMENTS

P.F.C is FRIA grant holder and J.C. a FNRS research fellow. The help of J.-M. Janot and P. Seta (LMPM, Mont-

pellier) in obtaining part of the experimental data is gratefully acknowledged. Thanks are due to the Fonds National de la Recherche Scientifique (FNRS/FRFC, Belgium) and the EU HCM Network ''Formation, Stability and Photophysics of Fullerenes'' (Contract No. ERBCHRXCT-940614) for financial support. The work in Mons is partly supported by the Belgian Federal Government ''Pôle d'Attraction Interuniversitaire en Chimie Supramoléculaire et Catalyse Supramoléculaire (PAI 4/11)'' and FNRS/FRFC. P.R.B. acknowledges the EPSRC for the award of an Advanced Fellowship.

[1] L. W. Tutt and A. Kost, Nature (London) **356**, 225 (1992).
[2] J. W. Arbogast, A. P. Darmanyan, C. S. Foote, M. M. Alvarez, S. J. Anz, and R. L. Whetten, J. Phys. Chem. **95**, 11 (1991).
[3] J. W. Arbogast and C. S. Foote, J. Am. Chem. Soc. **113**, 8886 (1991).
[4] Y.-P. Sun, in *Organic Photochemistry*, edited by V. Ramamurthy and K. S. Schanze (Marcel Dekker, New York, 1997), Vol. 1, p. 325.
[5] M. Maggini, G. Scorrano, M. Prato, G. Brusatin, A. Renier, R. Signorini, M. Meneghetti, and R. Bozio, Adv. Mater. **7**, 404 (1995).
[6] R. Signorini, M. Zerbetto, M. Meneghetti, R. Bozio, M. Maggini, C. De Faveri, M. Prato, and G. Scorrano, Chem. Commun. (Cambridge) **16**, 1891 (1996).
[7] Y.-P. Sun, G. E. Lawson, J. E. Riggs, B. Ma, N. Wang, and D. K. Moton, J. Phys. Chem. **102**, 5520 (1998).
[8] Y. Kojima, T. Matsuoka, H. Takahashi, and T. Kurauchi, J. Mater. Sci. Lett. **16**, 2029 (1997).
[9] Y. Song, G. Fang, Y. Wang, S. Liu, C. Li, L. Song, Y. Zhu, and Q. Hu, Appl. Phys. Lett. **74**, 332 (1999).
[10] R. V. Bensasson, E. Bienvenue, J.-M. Janot, S. Leach, P. Seta, D. I. Schuster, S. R. Wilson, and H. Zhao, Chem. Phys. Lett. **245**, 566 (1995).
[11] C. Luo, M. Fujitsuka, A. Watanabe, O. Ito, L. Gan, Y. Huang, and C.-H. Huang, J. Chem. Soc., Faraday Trans. **94**, 527 (1998).
[12] J. L. Anderson, Y.-Z. An, Y. Rubin, and C. S. Foote, J. Am. Chem. Soc. **116**, 9763 (1994).
[13] P. S. Baran, R. R. Monaco, A. U. Khan, D. I. Schuster, and S. R. Wilson, J. Am. Chem. Soc. **119**, 8363 (1997).
[14] H. Tokuyama, S. Yamago, E. Nakamura, T. Shiraki, and Y. Sugiura, J. Am. Chem. Soc. **115**, 7918 (1993).
[15] E. Nakamura, H. Tokuyama, S. Yamago, T. Shiraki, and Y. Sugiura, Bull. Chem. Soc. Jpn. **69**, 2143 (1996).
[16] T. Hamano, K. Okuda, T. Mashino, K. Arakane, A. Ryu, S. Mashiko, and T. Nagano, Chem. Commun. (Cambridge) **1**, 21 (1997).
[17] F. Diederich and C. Thilgen, Science **271**, 317 (1996).
[18] A. Hirsch, *The Chemistry of the Fullerenes* (Thieme, Stuttgart, 1994).
[19] R. Taylor and D. R. M. Walton, Nature (London) **363**, 685 (1993).
[20] D. M. Guldi, H. Hungerbühler, and K.-D. Asmus, J. Phys. Chem. **99**, 9380 (1995).
[21] D. M. Guldi and K.-D. Asmus, J. Phys. Chem. **101**, 1472 (1997).
[22] S.-K. Lin, L.-L. Shiu, K.-M. Chien, T.-Y. Luh, and T.-I. Lin, J. Phys. Chem. **99**, 105 (1995).
[23] B. Ma, C. E. Bunker, R. Guduru, X.-F. Zhang, and Y.-P. Sun, J. Phys. Chem. **101**, 5626 (1997).
[24] Y. Nakamura, T. Minowa, Y. Hayashida, S. Tobita, H. Shizuka, and J. Nishimura, J. Chem. Soc., Faraday Trans. **92**, 377 (1996).
[25] L. Udvardi, P. R. Surján, J. Kürti, and S. Pekker, Synth. Met. **70**, 1377 (1995).
[26] R. R. Williams, J. M. Zwier, and J. W. Verhoeven, J. Am. Chem. Soc. **117**, 4093 (1995).
[27] P.-F. Coheur *et al.*, Synth. Met. **103**, 2407 (1999).
[28] H. Mohan, D. K. Palit, J. P. Mittal, L. Y. Chiang, K.-D. Asmus, and D. M. Guldi, J. Chem. Soc., Faraday Trans. **94**, 359 (1998).
[29] D. K. Palit, H. Mohan, P. R. Birkett, and J. P. Mittal, J. Phys. Chem. **101**, 5418 (1997).
[30] G. Schick *et al.*, J. Am. Chem. Soc. **121**, 3246 (1999).
[31] K. Hutchison, J. Gao, G. Schick, Y. Rubin, and F. Wudl, J. Am. Chem. Soc. **121**, 5611 (1999).
[32] P. R. Birkett, A. G. Avent, A. D. Darwish, H. W. Kroto, R. Taylor, and D. R. M. Walton, J. Chem. Soc. Chem. Commun. **15**, 1230 (1993).
[33] A. G. Avent, P. R. Birkett, J. D. Crane, A. D. Darwish, J. G. Langley, H. W. Kroto, R. Taylor, and D. R. M. Walton, J. Chem. Soc. Chem. Commun. **12**, 1463 (1994).
[34] A. G. Avent, P. R. Birkett, and P. B. Hitchcock (unpublished).
[35] A. K. Rappé, C. J. Casewit, K. S. Colwell, W. A. Goddard III, and W. M. Skiff, J. Am. Chem. Soc. **114**, 10024 (1992).
[36] M. J. S. Dewar, E. G. Zoebisch, E. F. Healy, and J. J. P. Stewart, J. Am. Chem. Soc. **107**, 3902 (1985).
[37] M. J. Frisch, G. W. Trucks, H. B. Schlegel, P. M. W. Gill, B. G. Johnson, M. A. Robb, J. R. Cheeseman, T. Keith, G. A. Petersson, J. A. Montgomery, K. Raghavachari, M. A. Al-Laham, V. G. Zakrzewski, J. V. Ortiz, J. B. Foresman, J. Cioslowski, B. B. Stefanov, A. Nanayakkara, M. Challacombe, C. Y. Peng, P. Y. Ayala, W. Chen, M. W. Wong, J. L. Andres, E. S. Replogle, R. Gomperts, R. L. Martin, D. J. Fox, J. S. Binkley, D. J. Defrees, J. Baker, J. P. Stewart, M. Head-Gordon, C. Gonzalez, and J. A. Pople, GAUSSIAN 94, revision E.1, Gaussian Inc., Pittsburgh, 1995.
[38] J. P. Stewart, *Mopac 93.00 Manual* (Fujitsu, Tokyo, 1993).
[39] M. J. S. Dewar and W. Thiel, J. Am. Chem. Soc. **99**, 4899 (1977).
[40] R. S. Mulliken, J. Chem. Phys. **33**, 1833 (1955).
[41] T. Koopmans, Physica (Amsterdam) **1**, 104 (1933).
[42] M. C. Zerner, G. H. Loew, R. F. Kichner, and V. T. Mueller-Westerhoff, J. Am. Chem. Soc. **102**, 589 (1980).
[43] N. Mataga and K. Nishimoto, Z. Phys. Chem. (Frankfurt am Main) **13**, 140 (1957).
[44] R. J. Bell, P. Dean, and D. C. Hibbins-Buttler, J. Phys. C **3**, 2111 (1970).
[45] D. A. dos Santos, C. Quattrochi, R. H. Friend, and J. L. Brédas, J. Chem. Phys. **100**, 3301 (1994).
[46] INSIGHTII *User Guide, Molecular Simulations* (1996).
[47] R. D. Bendale, J. D. Baker, and M. C. Zerner, Int. J. Quantum Chem., Symp. **25**, 557 (1991).
[48] R. D. Bendale and M. C. Zerner, J. Phys. Chem. **99**, 13830 (1995).
[49] M. Braga, S. Larsson, A. Rosén, and A. Volosov, Astron. Astrophys. **245**, 232 (1991).
[50] J. Feng, J. Li, Z. Wang, and M. C. Zerner, Int. J. Quantum Chem. **37**, 599 (1990).
[51] J. Feng, J. Li, Z. Li, and M. C. Zerner, Int. J. Quantum Chem. **39**, 331 (1991).
[52] S. Larsson and A. Volosov, Chem. Phys. Lett. **137**, 501 (1987).
[53] F. Negri and G. Orlandi, Chem. Phys. Lett. **144**, 31 (1988).
[54] F. Negri, G. Orlandi, and F. Zerbetto, J. Chem. Phys. **97**, 6496 (1992).
[55] F. Negri and G. Orlandi, Z. Phys. Chem. (Wiesbaden) **200**, 85 (1997).
[56] A. Sassara, G. Zerza, M. Chergui, F. Negri, and G. Orlandi, J. Chem. Phys. **107**, 8731 (1997).
[57] I. Lazlo and L. Udvardi, Chem. Phys. Lett. **136**, 418 (1987).
[58] I. Lazlo and L. Udvardi, Int. J. Quantum Chem. **42**, 1651 (1992).
[59] M. C. Zerner, in *Reviews in Computational Chemistry*, edited by K. B. Lipkowitz and D. B. Boyd (VCH, New York, 1995), Vol. 2, p. 313.
[60] E. W. Godly and R. Taylor, Pure Appl. Chem. **69**, 1412 (1997).
[61] R. Taylor, Tetrahedron Lett. **32**, 3731 (1991).
[62] R. Taylor, J. Chem. Soc., Perkin Trans. 2 **1**, 3 (1992).
[63] R. Taylor, Philos. Trans. R. Soc. London, Ser. A **343**, 87 (1993).
[64] W. I. F. David *et al.*, Nature (London) **353**, 147 (1991).
[65] J. Cioslowski, *Electronic Structure Calculations on Fullerenes and their Derivatives* (Oxford University Press, Oxford, 1995).
[66] H. Iikura, S. Mori, M. Sawamura, and E. Nakamura, J. Org. Chem. **62**, 7912 (1997).
[67] D. L. Lichtenberger, K. W. Nebesney, C. D. Day, D. R. Huffman, and L. D. Lamb, Chem. Phys. Lett. **176**, 203 (1991).
[68] L.-S. Wang, J. J. Conceicao, C. M. Jin, and R. E. Smalley, Chem. Phys. Lett. **182**, 5 (1991).
[69] P.-F. Coheur *et al.*, J. Chem. Phys. (in press).
[70] P.-F. Coheur *et al.*, in *Recent Advances in the Chemistry and Physics of Fullerenes and Related Materials*, edited by K. M. Kadish and R. S. Ruoff (The Electrochemical Society Inc., Pennington, 1998), Vol. 6, p. 1156.
[71] In Fig. 4 the fluorescence signal around 650 nm is likely to be due to a fraction of the pseudosymmetrical $C_{60}Ph_5OH$ isomer 1 in the sample.
[72] A. Sassara, G. Zerza, and M. Chergui, J. Phys. B **29**, 4997 (1996).
[73] R. V. Bensasson, E. Bienvenue, M. Dellinger, S. Leach, and P. Seta, J. Phys. Chem. **98**, 3492 (1994).
[74] Electrochemical studies of these and other derivatives are being undertaken in collaboration with F. Paolucci and F. Zerbetto.
[75] S. Leach *et al.*, Chem. Phys. **160**, 451 (1992).
[76] D. Kim, M. Lee, Y. D. Suh, and S. K. Kim, J. Am. Chem. Soc. **114**, 4929 (1992).